

# A Behavioral Handwriting Model for Static and Dynamic Signature Synthesis

Miguel A. Ferrer, Moises Diaz, Cristina Carmona-Duarte and Aythami Morales

**Abstract**—The synthetic generation of static handwritten signatures based on motor equivalence theory has been recently proposed for biometric applications. Motor equivalence divides the human handwriting action into an effector dependent cognitive level and an effector independent motor level. The first level has been suggested by others as an engram, generated through a spatial grid, and the second has been emulated with kinematic filters. Our paper proposes a development of this methodology in which we generate dynamic information and provide a unified comprehensive synthesizer for both static and dynamic signature synthesis. The dynamics are calculated by lognormal sampling of the 8-connected continuous signature trajectory, which includes, as a novelty, the pen-ups. The forgery generation imitates a signature by extracting the most perceptually relevant points of the given genuine signature and interpolating them. The capacity to synthesize both static and dynamic signatures using a unique model is evaluated according to its ability to adapt to the static and dynamic signature inter- and intra-personal variability. Our highly promising results suggest the possibility of using the synthesizer in different areas beyond the generation of unlimited databases for biometric training.

**Index Terms**— Biometric recognition, on-line and off-line synthetic generation, signature verification, motor equivalence theory, kinematic theory of human movement.



## 1 INTRODUCTION

A handwritten signature is the final response to a complex cognitive and neuromuscular process which is the result of the growing up and learning functions. This starts during childhood with lines and scribbles. Later, young children begin to use letters in their own style, although their motor control is usually not very accurate. Tracing helps both to improve their motor control and the learning of the shape and spatial relationships between objects, thus creating the spatial memory or cognitive map. Once this knowledge is acquired and the motor skills begin to mature, it is possible to select an ordered sequence of target points to perform fluent and effortless handwriting. At this stage, the person is ready to define and practice his or her own signature [1].

Although signature definition, which is the basis of inter-personal variability, is barely modified, its execution changes continuously due to long and short term factors. The long term drifting is mainly caused by aging whereas short term variability is due to either psychological reasons or external factors such as different stances, writing tools, signing surfaces, or other unaccountable reasons. Modeling these variabilities is a key factor in signature analysis and it is treated differently in several scientific fields.

For instance, automatic signature verification for personal identification [2][3] looks for features with both

inter-personal discriminative ability and intra-personal stability. These features are extracted from either the static signature image or the signature dynamics [4][5]. Forensic analysis examines the authenticity of inked signatures by careful visual inspection of features such as the caliber, proportion, spacing, progression, pressure, gesture and the area occupied by the signature. This is to detect forgeries and illegitimate changes [6].

In the field of health, handwriting can also be applied to the identification of some learning problems for children or early stage degenerative cognitive or motor problems [7]. In this connection, rapid hand movement velocity profiles made during the handwriting process have been studied in depth [8]. Such models are currently being used in many applications such as identifying factors responsible for brain strokes [9][10] and diagnosing and preventing neurodegenerative diseases, such as Parkinson's [11] and Alzheimer's [12] among others. Also graphology uses handwriting to estimate, for instance, general personality traits, intelligence, social skills, emotions and social attitudes [13].

A common problem for researching in the above areas is the lack of handwritten signature samples. Their collection is costly. Besides, the design of a new database is usually focused on solving a well-defined problem which limits application to other areas. Additionally, legal issues regarding data protection hamper the sharing and distribution of biometric data [14].

The generation of synthetic handwritten signature data has emerged to alleviate these drawbacks and to better understand the cognitive and muscular processes involved in handwriting. Synthetic datasets can be used for

1. Miguel A. Ferrer, Moises Diaz and Cristina Carmona-Duarte are with Instituto Universitario para el Desarrollo Tecnológico y la Innovación en Comunicaciones, Universidad de Las Palmas de Gran Canaria, Las Palmas de Gran Canaria, Spain. Emails: mferrer@idetic.eu, mdiaz@idetic.eu, ccarmona@idetic.eu
2. Aythami Morales is with ATVS-Biometric Research Group, Universidad Autónoma de Madrid, Spain. Email: aythami.morales@uam.es

xxxx-xxxx/0x/\$xx.00 © 200x IEEE

Published by the IEEE Computer Society

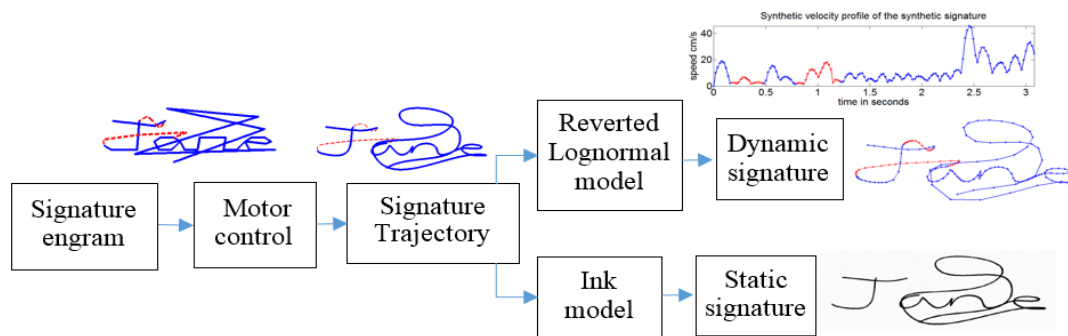


Fig. 1. Block diagram of the dual static and dynamic signature generation procedure. Solid blue lines show the pen-downs of the signature trajectory whereas solid red lines refer to pen-ups. Dots on the blue lines indicate signature sampling points.

preliminary algorithm assessment without the economic and time cost of developing real datasets. Additionally, these synthetic data can be shared without legal concerns.

### 1.1 Related work

There are various proposals in the literature for generating synthetic handwritten signatures. Some of them generate duplicates of a given signature. Duplicates can be generated by simple affine distortion or stroke wise distortion as in [15] for static and in [16] for dynamic signature verification. The method proposed at [17][18][19], based on the sigma lognormal model, is also useful for signature duplication. In [20] new static signatures are generated from two dynamic samples from the same user while in [21] a cognitive model is proposed for duplicating off-line signatures from one dynamic sample.

The popular glyph-based methods for handwriting synthesis, which record separate letters or words from one user and join them after applying geometric deformation to simulate new handwriting [22][23][24][25], has not been used for signature synthesis, as far as we know.

Another research line is model-based handwriting synthesis which generates new synthetic identities. The Popel approach in [26] describes a signature generation model based on visual characteristics extracted from the time domain. Another methodology is proposed by Galbally et al. in [27][28] for the generation of synthetic on-line signatures on the basis of the flourish. This method combines the advantages of both spectral analysis and the kinematic theory of rapid human movements [29][30][31][32] to generate the dynamic signature of a new identity. Similarly, a proposal to use heuristic procedures to generate genuine and forged off-line flourish-based signatures is proposed at [33]. A human like model for generating off-line signatures with both the flourish and text of new identities is proposed at [34] which is inspired by the motor equivalence model [35].

Summing up, different models have been proposed but there is no flexible method to generate different signatures of new identities containing both text and flourish in both static and dynamic versions from a unified synthesizer. This paper is aimed to fill this gap and takes steps significantly beyond our previous work at [34].

### 1.2 Our proposal

This paper develops a human like model for signature synthesis inspired by motor equivalence theory [35]. The signature synthesizer includes synthetic signature definition with text and flourish, the generation of genuine signatures and of forgeries with both static and dynamic patterns. Pen-ups are also included. The databases generated with this synthesizer produce simultaneously coherent performance results in the static and dynamic domains. As far as we know, this is the only signature synthesizer that includes all these features.

The neuromotor equivalence theory [7] divides human physical action into two steps: the cognitive plan and motor control. Specifically, the movement is encoded in the central nervous system as a plan [35], independent of commands to specific muscles. For example, handwriting may be represented in terms of strokes which are encoded as relative positions and spatial directions [35]. Once the movement has been planned, motor control delivers the commands to specific muscles to produce the handwriting [36]. As [37] suggests, fast and coordinated movements cannot be executed solely under feedback control since biological feedback is slow. Therefore, the brain needs to acquire by motor learning an inverse model of the object to be controlled.

The procedure proposed in this paper, which is illustrated at Fig. 1, can be summarized as follows: first, the synthetic user signature morphology is defined (Section 2). Second, we define a user grid, based on the cognitive map (Section 3). Third, we represent the name and flourish engrams as a sequence of grid nodes and their stroke limits, including pen-ups (Section 3). Fourth, we design the signature trajectory by applying a motor model to the signature engram (Section 4). Fifth, from the signature trajectory, we generate the dynamic signature by lognormal sampling of the signature trajectory (Section 5). Finally, we generate multiple samples and forgeries (Section 6) that mimic the performance of real databases (Section 7).

As result of these developments, human like realistic signatures are generated. These could be useful for the aforementioned scientific areas, beyond just compiling datasets for biometrics. Obviously, the fact that this signature synthesis has been developed using neuroscience concepts does not mean that we claim any

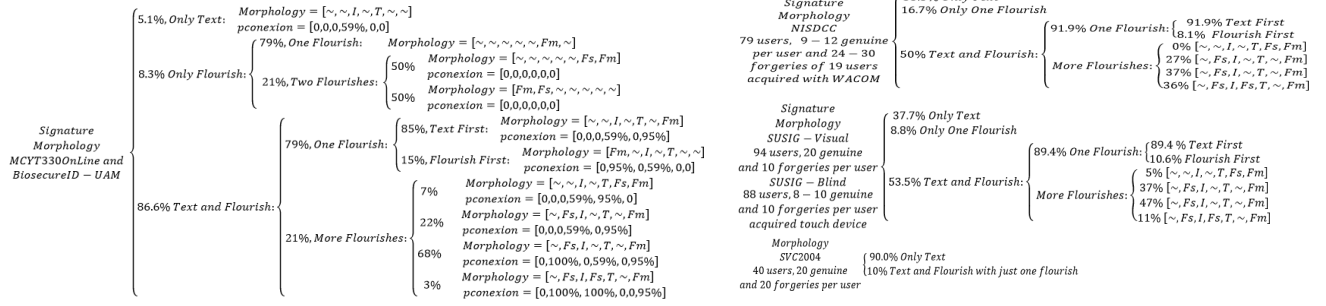


Fig. 2. Database morphology for synthetic identity generation

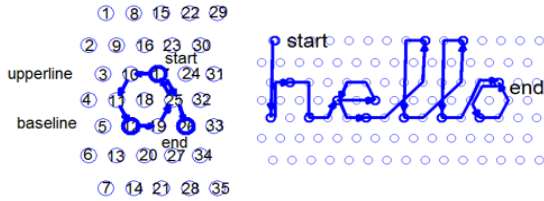


Fig. 3. Engram of the body letter 'a' on the hexagonal letter grid (left). Engram of the word 'hello' on the tessellation (right). The stroke limits are the grid nodes marked with the wider edges

fidelity to cognitive and neuromotor processes underlying handwriting production.

## 2. GENERATING SYNTHETIC IDENTITIES

Generating a synthetic identity is equivalent to designing the signature morphology which is the language model needed to generate readable synthetic names, the signature components such as text and flourish and the relation between them such as the components' order and connection rules [34][38].

Specifically, this paper considers the following components in a synthetic signature. *I*: capital initial letter of the text, *T*: text of the readable part of the signature, *Fm*: main flourish and *Fs*: secondary flourish. Possible sequences of these elements are defined by means of a vector called *Morphology* = [*Fm*, *Fs*, *I*, *Fs*, *T*, *Fs*, *Fm*].

The connections are defined in the vector *Connection*. If *Connection*(*k*) = 1, then the component *Morphology*(*k* + 1) is connected to the previous component, otherwise it is disconnected. For instance, a signature with a small flourish at the very beginning followed by a connected initial, a space and the rest of the name connected with a flourish is defined as *Morphology* = [~., *Fs*, *I*, ~., *T*, ~., *Fm*] and *Connection* = [0, 1, 0, 0, 1].

The components of these vectors were worked out randomly from different probability density functions. These functions were determined manually from each one of the following datasets: MCYT330OnLine Signature [39], BiosecureID-Signature UAM subcorpus [40], NISDCC [41][42], SVC 2004 [43], and the two SUSIG subcorpus: Blind and Visual [44] the characteristics of all of which are shown at Fig. 2.

Likewise, the number of words per signature and letters

per word, the slant, skew, number of corners of the main and secondary flourishes, velocity for the production of genuine signatures and forgeries, stroke time dispersion, text to flourish width ratio and flourish to text center ratio have also been modeled for each dataset [38]. These values are worked out randomly for each synthetic user.

The text of the synthetic signatures is based on a simple language model which alternates consonants and vowels. The probability of repeating a consonant and a vowel is fixed at 0.95. The probability of using any letter is obtained from its frequency of appearance in the English language. So we obtain realistic texts which are readable but avoid real names because of potential privacy concerns.

## 3. THE COGNITIVE PLAN: SIGNATURE ENGRAM

Once the signature morphology is defined, the action plan for writing the signature is calculated. This is carried out by generating a signature engram which imitates the cognitive action plan of motor equivalence theory [7][35].

This theory suggests [7] that actions are encoded in the central nervous system as a plan [35]. How the cortex encodes information about position (i.e. place, distance and direction) in cortical microcircuits is poorly understood. Hafting et al. [45] show that the dorsocaudal medial entorhinal cortex (DMEC) contains a directionally oriented, topographically organized neural map of the spatial environment. Its key unit is the grid cell which is activated whenever the person's position coincides with any vertex of a regular grid of equilateral triangles spanning the surface of the environment. Hafting et al. suggest [45] that a place code is computed in the entorhinal cortex and fed into the hippocampus, which may make the associations between place and events that are needed for the formation of memories.

Inspired by this idea, the signature engram is defined as a sequence of nodes through a hexagonal grid that spans the signing surface. The hexagonal grid is defined by the distance between rows and columns. For each signer these values are randomly defined between a maximum and minimum heuristically selected, as shown in Fig. 3.

The signature engram is described in three steps: text, pen-ups and flourish engrams.

### 3.1 Text engram

In our implementation, the engram sequences of every

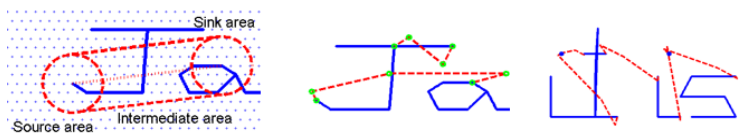


Fig. 4. Left: Areas for pen-up engram definition. Center: pen-up engram linking two letters. The grid nodes selected are marked by green circles. Right: Text with diacritic marks which are written along with the following pen-up. Letters in continuous blue lines and pen-ups in dashed red lines.

Fig. 5. Signature envelope on the grid span, flourish and text engram →

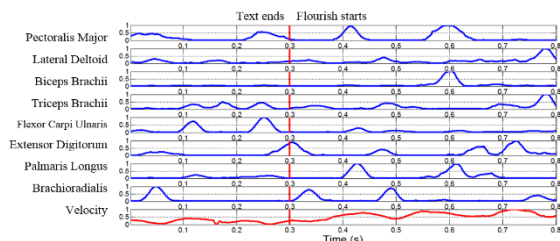
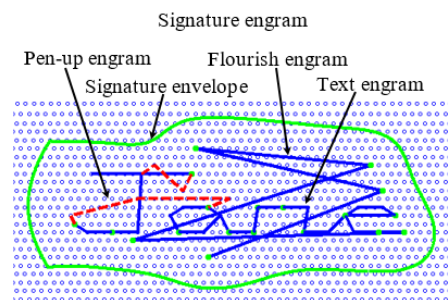


Fig. 6. Activity of several arm muscles in the transition from text to flourish of a real user while signing.

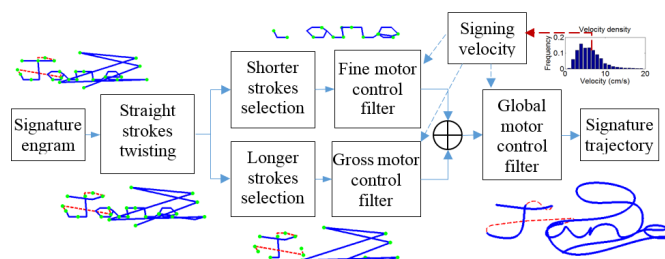


Fig. 7. Multi-level motor control model inspired by inverse internal models. Solid blue line: written signature, dashed red lines: pen-ups, green circles: stroke limits.

Latin alphabet letter have been defined in three parts: prefix, body and suffix. The prefix means a ligature added to the beginning to connect the body with the previous letter. The body defines the individual isolated letter and the suffix also connects the body to the next letter. If the body of the letter is not connected, the prefix and suffix are not used. Different prefixes, bodies and suffixes for each letter were generated.

Each letter engram definition includes a stroke division which means the nodes where the pen velocity will be the minimum in the synthetic velocity profile. These were defined by inspecting recorded samples of each letter and examining minima in the velocity profile. Some stroke division nodes can be seen at Fig. 3 as the nodes with wider borders. Note that these trajectory points are not necessarily related to the cortex action plan. This procedure is loosely based on equivalence model theory but it does not pretend to model it.

### 3.2 Pen-up engrams

Once the text engrams are defined, it is necessary to define the pen-up engrams, i.e. the trajectory which represents the pen being lifted between written strokes. Pen-up trajectories can be divided into three zones: the start or source area, the intermediate area and the sink area.

1. The source area is located around the end of the previously written stroke. When the pen is lifted, sometimes it displays a degree of hesitation until it begins the transition to the start of the next stroke.
2. The intermediate area is defined by the trajectory from the source area to the sink area.
3. The sink area is located around the beginning of the next written stroke. Just before the pen starts to write, a randomly made decision about the precise point at

which to start creates variability for the end of the trajectory in that area.

The proposed pen-up model defines the source area as a circle around the end of the first stroke. After manually examining many pen-up trajectories in different databases, its radius is heuristically set to  $d/10$ ,  $d$  being the pen-up distance. The sink area is a similar circle, centered on the beginning of the second stroke. The intermediate area is a rectangle that links the source and sink areas. The model is illustrated at Fig. 4.

A number of grid nodes are randomly selected inside each area. The number of nodes defines the hesitation after lifting the pen. The more nodes, the more hesitation has occurred. Heuristically, to choose one or two nodes per area is usually sufficient to obtain realistic pen-up trajectories. An example of a pen-up engram linking a disconnected stroke with a node area is shown at Fig 4.

The letters with delayed strokes, due to a diacritical mark, e.g. the "i" or "t", require a pen-up when they are written. After analyzing the parameterized human behavior in the available databases, the synthesizer writes the delayed stroke after the next pen-up which could be due to a non-connected letter or word ending. When several diacritical marks have to be written, they are written from left to right. An example is shown at Fig. 4.

### 3.3 Flourish engram

Once the text engram is defined, the tessellation is spanned to include the flourish nodes. The flourish engram is defined as a sequence of grid nodes inside a generated envelope, which limits and shapes the spanning area. Consequently, the signature envelopes do not affect the generation of signatures without a flourish.



The envelope is synthesized for each signer by means of an Active Shape Model (ASM) [46]. Keeping to a more general envelope model, the ASM has been trained with the MCYT75OffLine database [39] which is the database with the most signatures with flourishes and different text-flourish configurations.

The mass center of the ASM envelope is displaced to match the geometrical center of the text engram. Then it is scaled to fit the text to flourish width ratio and displaced to fix the flourish to text center ratio.

The nodes of the flourish engram are then obtained by randomly selecting the nodes inside the envelope, with the following two conditions: 1) the lines that link the nodes are not allowed to intersect the signature envelope; and 2) the vertex angle of each node is less than  $90^\circ$ . In this way, the flourish corners are considered stroke limits. If the text and flourish are connected, the end of the text engram and the beginning of the flourish engram are linked. The whole engram generation process is illustrated in Fig 5.

#### 4. MOTOR CONTROL: SIGNATURE TRAJECTORY

Once the signature engram is defined, an inverse model for motor control is applied to obtain a realistic human signature ballistic trajectory. To achieve this, the engram nodes are linked by 8-connected Bresenham's lines and inertial moving average filters are applied to these lines.

The way the filters are applied to the engram is worked out after recording and analyzing the electromyographic (EMG) signals of six volunteers while they were writing a signature. The normalized muscle activity RMS curves were obtained by using a similar procedure to that in [47]. For example, Fig. 6 shows the RMS curves per muscle of one of the volunteers while signing.

After undertaking a clustering study of muscle activity, based on k-means, it became clear that there are three basic ensembles of muscles, the activity of which depends on the kind of handwritten stroke. The first ensemble is active during the whole signing process, the second ensemble is more active during the handwriting of short strokes whereas the third ensemble is more active during the longer strokes.

This conclusion leads us to a multilevel motor scheme which is modeled by motor inertial filters as follows: i) a so-called fine motor control filter is applied to the shorter strokes which are the slowest ones with lesser inertia, ii) a so-called gross motor control filter is applied to the longer strokes which are the fastest with greater inertia and iii) the whole signature is filtered by the so-called global motor control filter. This procedure is illustrated at Fig. 7.

Specifically, the signature trajectory is worked out as follows: The fine motor control filter is applied to the line segments belonging to the shorter strokes and stops at every stroke limit. The gross motor control filter is applied to the rest of the engram and stops at each pen-up and pen-down. The result is filtered by the global motor control filter to obtain the ballistic trajectory, as shown at Fig. 7.

We used Kaiser filters with a symmetric finite impulse

response  $h(n)$  defined as:

$$h(n) = \begin{cases} I_0(\pi\beta\sqrt{1 - (2n/N - 1)^2}) & 0 \leq n \leq N \\ 0 & \text{otherwise} \end{cases} \quad (1)$$

where  $N$  corresponds to the filter length and  $\beta$  is the shape factor. The value of  $\beta$  is chosen randomly between  $[0, 0.5]$ . The value of  $N$  is related to the signing velocity: the higher the signature velocity, the longer is the filter  $N$  value.

The signature velocity is obtained by randomly following its probability density function, modeled as a generalized extreme value (GEV) distribution defined by:

$$f(x; \mu, \sigma, \xi) = \frac{1}{\sigma} t(x)^{\xi+1} \exp\{-t(x)\} \quad (2)$$

$$\text{where } t(x) = \begin{cases} \left(1 + \frac{x-\mu}{\sigma}\xi\right)^{-1/\xi} & \text{if } \xi \neq 0 \\ \exp\left\{-\frac{x-\mu}{\sigma}\right\} & \text{if } \xi = 0 \end{cases} \quad (3)$$

The values of the GEV parameters  $\mu, \sigma, \xi$  are estimated by maximizing their likelihood given the velocity of all the signatures for all the above mentioned databases (see Section 2). The velocity of each signature is calculated as the total length of the trajectory divided by the signing time. The worked out values for genuine signatures are  $\mu = 0.10, \sigma = 2.20$  and  $\xi = 4.72$  and for the forgeries  $\mu = 0.19, \sigma = 1.74$  and  $\xi = 3.08$ . As the GEV distributions run from  $-\infty$  to  $+\infty$ , minimum and maximum values are established for these distributions:  $v_{min} = 1.50 \text{ cm/s}$  and  $v_{max} = 10.0 \text{ cm/s}$  for genuine signatures and  $v_{min} = 0.85 \text{ cm/s}$  and  $v_{max} = 15.0 \text{ cm/s}$  for forgeries. Thus, let  $v_s$  be the randomly worked out signature velocity through the GEV distribution, the length for fine, gross and global inertia filters are obtained as  $N_f = I_f \times v_s, N_g = I_g \times v_s$  and  $N_w = I_w \times v_s$ ,  $I_f$  and  $I_g$  respectively being the distance between the grid nodes of the synthetic user, whereas  $I_w$  is the averaged distances between the flourish nodes.

A drawback of this procedure is that the ballistic trajectory of straight strokes appears unnaturally written. This occurs mainly to the capital letters. This problem is alleviated by twisting the Bresenham's line of longer straight strokes before filtering. The twisting consists in converting the straight lines to triangles. The triangle height is a constant for each writer in the heuristic range  $[0, d/10]$ ,  $d$  being the length of the straight stroke. An example of the results can be seen at Fig. 7 for the capital letter "J".

After filtering, the static image of the signature is obtained by applying an ink deposition model of a ballpoint pen to the trajectory [34][48].

#### 5. SIGNATURE DYNAMICS

The dynamic information of the signature is obtained by lognormal sampling of the continuous trajectory. The kinematic theory suggests that the velocity of rapid strokes [29][30][31][32] can be modeled by a delta-lognormal. Each lognormal is characterized by its amplitude  $D$ , time of occurrence  $\tau$ , the log time delays  $\mu$  and the log-response time  $\sigma$ . The velocity profile of a stroke is then:

$$v(t) = D_1 \Lambda(t; \tau_1, \mu_1, \sigma_1^2) - D_2 \Lambda(t; \tau_2, \mu_2, \sigma_2^2) \quad (4)$$

where

$$\Lambda(t; \tau, \mu, \sigma^2) = \frac{1}{\sigma \sqrt{2\pi}(t - \tau)} \exp \left\{ -\frac{[\ln(t - \tau) - \mu]^2}{2\sigma^2} \right\} \quad (5)$$

, for  $t > \tau$ , and 0 otherwise

Therefore, a means of generating realistic signature dynamic information is to sample the continuous signature trajectory in such a way that the reconstructed velocity profile closely matches a lognormal shape.

This can be performed as follows: suppose that the temporal velocity of the stroke  $v(t)$  is described by just one lognormal (the agonist), since  $D_2 \approx D_1/10$  [32] then:

$$v(t) = \frac{D}{\sigma \sqrt{2\pi}(t - \tau)} \exp \left\{ -\frac{(\ln(t - \tau) - \mu)^2}{2\sigma^2} \right\} \quad (6)$$

The distance at time  $t$  is given by the lognormal cumulative function:

$$e(t) = \int_{-\infty}^{\infty} v dt = \frac{D}{2} \left( 1 + \operatorname{erf} \left( \frac{\ln(t - \tau) - \mu}{\sqrt{2}\sigma} \right) \right) \quad (7)$$

Solving for  $t$  in the equation, the time in terms of the distance is given by:

$$t(e) = \exp \{ \sqrt{2}\sigma \operatorname{erf}^{-1}(2e/D - 1) + \mu \} \quad (8)$$

and the velocity in terms of distance can be worked out by substituting Eq. (8) into Eq. (6), thus obtaining:

$$v(e) = \frac{D \exp \{ -\sqrt{2}\sigma \operatorname{erf}^{-1}(2e/D - 1) \}}{\sigma \sqrt{2\pi} \exp \{ \sqrt{2}\sigma \operatorname{erf}^{-1}(2e/D - 1) + \mu \}} \quad (9)$$

So the sampling procedure selects the pixels at  $e(nT_s)$  with Eq. (7),  $f_s = 1/T_s$  being the sampling frequency. But Eq. (7) requires us to define the amplitude  $D$ , the log-time delay  $\mu$  and the log-response time  $\sigma$  for each stroke. Firstly, these were obtained as random values inside the margins given at [8] but the results were not perceptually realistic.

Consequently, the skewness and kurtosis of all the individual lognormals were studied from the signatures of the aforementioned databases with ScriptStudio [49]. The results give an averaged skewness and kurtosis of 0.13 and 3.08 respectively which shows that the lognormals are generally located around the temporal center of the strokes because the kurtosis is close to 3. Moreover, a low positive skew to the left is observed since the skewness is near zero but positive.

Additionally, for every stroke it is possible to calculate its length and time. The temporal duration of the whole signature can be calculated by dividing the signature length by the signature velocity, as worked out in section 4. The time taken for each stroke is obtained from the existence, as suggested by Neuroscience, of the so called Central Pattern Generator (CPG) [36] which produces rhythmic patterned outputs without sensory feedback. Moreover, it has been suggested that the mammalian locomotor CPG comprises a "timer" which generates step cycles of varying duration and a pattern formation layer

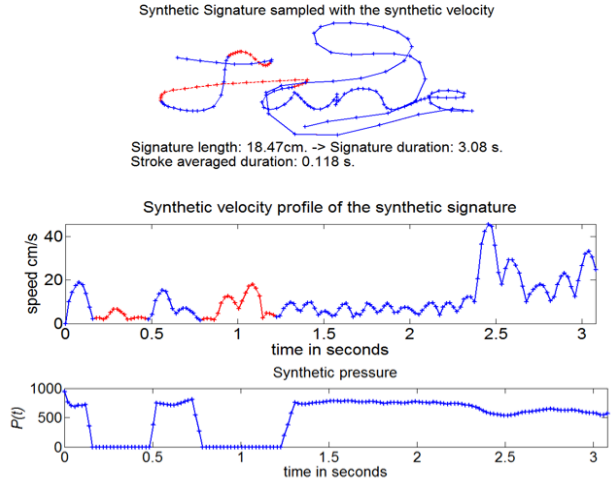


Fig. 8. Synthetic dynamic version of the static signature of "Jane".

which selects and grades the activation of motor pools [36]. Therefore, if the stroke generation is simulated by the CPG step cycle, the duration of each stroke should be very similar. This has been verified using the MCYT330OnLine signature database for which the dispersion of the temporal duration of strokes has been modeled as a GEV distribution with the parameters:  $\mu = -0.21$ ,  $\sigma = 0.06$ ,  $\xi = 0.29$ ,  $t_{\min} = 0.15$  and  $t_{\max} = 0.50$ . Consequently, the duration assigned to each stroke of the synthetic signature is worked out by dividing the whole signature duration by the number of strokes thus leading to the dispersion.

### 5.1 Lognormal sampling

Once the stroke length  $l_s$  is known and its time  $t_s$ , its lognormal parameters can be obtained as follows. From Eq. (7) we deduce:

$$l_s = \frac{D}{2} \left( 1 + \operatorname{erf} \left( \frac{\ln t_s - \mu}{\sqrt{2}\sigma} \right) \right) \quad (10)$$

As  $\operatorname{erf}(3) = 1$ , a possible solution of Eq. (10) is

$$D = l_s \quad (11)$$

$$\mu = \ln t_s - 3\sqrt{2}\sigma \quad (12)$$

Furthermore, as the lognormals are centered in the middle of the stroke with a low positive skew, their maximum or mode, defined by  $e^{\mu - \sigma^2}$ , is around  $t_s/2$  with a slight left skew. Therefore, it holds that:

$$kt_s = e^{\mu - \sigma^2}, 0.4 < k < 0.5 \quad (13)$$

Combining Eq. (12) and Eq. (13) we obtain:

$$\sigma^2 + 3\sqrt{2}\sigma - \ln k = 0 \quad (14)$$

Thus, in the case of an isolated stroke of length  $l_s$  and duration  $t_s$ , the simplified approach lets us work out the lognormal parameters  $D$  as equal to  $l_s$  (see Eq. (11)),  $\sigma$  as the positive solution of the simple second order Eq.(14), and  $\mu$  by substituting  $\sigma$  in Eq. (12). This procedure is useful only for isolated strokes.

In the case of a sequence of overlapping strokes, the parameters of each individual stroke are worked out

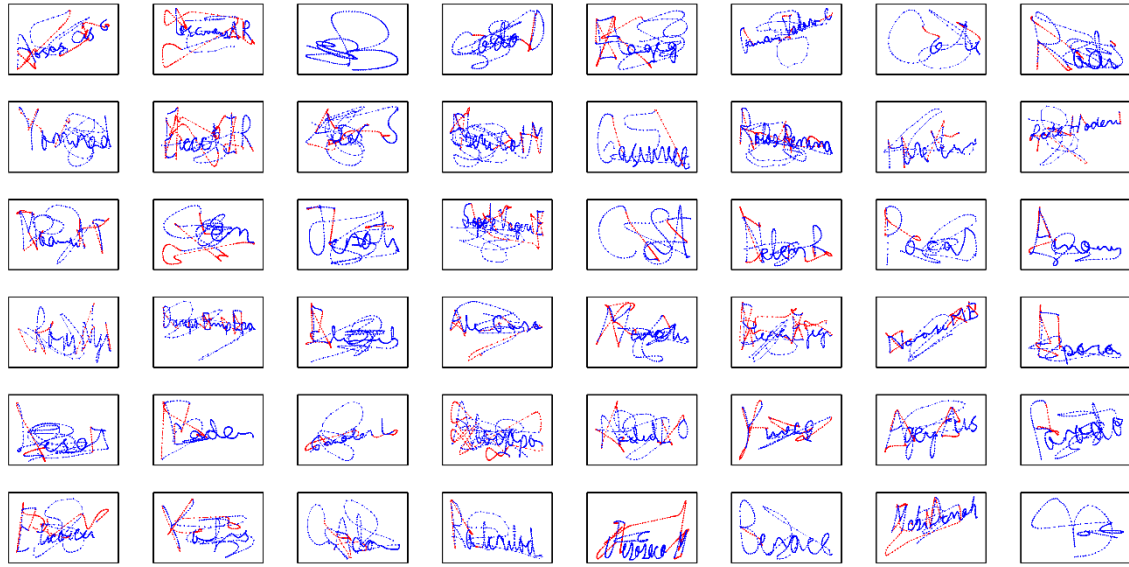


Fig. 9. Examples of dynamic signatures synthetically generated. Blue dots show pen-downs samples whereas red dots refer to pen-ups samples.

separately by assuming that the overlapping doubles the length of each stroke. Then, from Eq. (9), the spatial velocity  $v(e)$  of each stroke is obtained and the signature velocity profile is calculated by summing the velocity of all the strokes, as in the case of the sigma lognormal model [49] but in the spatial domain instead of the temporal.

The synthetic signature trajectory is then sampled from  $v(e)$  as follows. Let be  $x_e$  and  $y_e$  the coordinates of the 8-connected signature trajectory at a resolution of  $r$  dots per inch. The distance between samples in centimeters is worked out as:

$$d(e) = 2.54 \left( \sqrt{(x_e - x_{e-1})^2 + (y_e - y_{e-1})^2} \right) / r \quad (15)$$

Consequently, the time the pen is over each signature spatial pixel is obtained as  $t(e) = d(e)/v(e)$ . If  $t(e) > 1/f_m$  then it is set to  $t(e) = 1/f_m$ . Finally, the accumulated time along the signature trajectory is worked out and the trajectory is sampled by selecting the pixels for which the time is closer to multiples of  $1/f_m$ ,  $f_m$  being the sample frequency. The accuracy of the signature trajectory sampling is estimated by comparing real and synthetic velocity profiles reconstructed from the signature trajectory. The SNR between both synthetic and real velocity profiles is 15.9 dB for the MCYT330Online.

Summing up, from the synthetic signature trajectory which includes the stroke limits, we get each stroke length and temporal duration. Then, through Eq. (11), Eq. (12) and Eq. (14) we obtain the  $D$ ,  $\mu$  and  $\sigma$  lognormal parameters of each stroke and their spatial velocity profiles from Eq. (9) which are summed to build the whole signature spatial velocity profile. Knowing the velocity at each pixel, the time is also known, and the signature trajectory can be sampled. Fig. 8 shows the realism of the synthetic dynamic information. We should mention that the values obtained for  $D$ ,  $\mu$  and  $\sigma$  lie within the parameters margins given at [8].

## 5.2 Pen pressure modelling

The pressure has been modeled as inversely proportional to the velocity, even though this is only partially true. Specifically, the pressure,  $p(t)$ , is obtained by inverting the normalized A-law compressed velocity  $vc(e)$  and translating it into the range of a WACOM commercial dynamic acquisition device which is  $[500 + U, 850 + U]$ , where  $U$  is a random variable with uniform distribution between  $[0, 150]$  worked out for each user. This procedure is formulated at Eq. (16).

$$p(t) = \begin{cases} 0 & \text{if pen - ups} \\ 2U \frac{VC - vc(e)}{VC} + 500 + U & \text{otherwise} \end{cases} \quad (16)$$

where  $VC$  is the maximum of  $vc(e)$ . Obviously, during the pen-ups,  $p(t)$  is set to zero. Following the WACOM pressure signal, the transition between pen-up/pen-down is found to be linear and 2 or 3 samples long. Fig. 8 shows an example of a pressure profile.

## 6 GENERATION OF MULTIPLE SAMPLES FOR A GIVEN IDENTITY

The above procedures define the morphology, cognitive and motorial parameters for making the master signature of a synthetically defined identity. As an example, Fig. 9 shows several fully synthetic signatures.

The next step is to generate the intra-personal variability, i.e. by getting different samples each time the algorithm is executed. This section also addresses the generation of synthetic forgeries by mimicking the human procedure used for copying a signature.

### 6.1 Multiple sample generation

According to the generation methodology proposed in this work, a master signature is defined by the set of  $\varphi$  morphological, static and dynamic parameters defined in Sections 2, 3 and 4. The intra-personal variability is performed with so called variability variables  $vv$  that

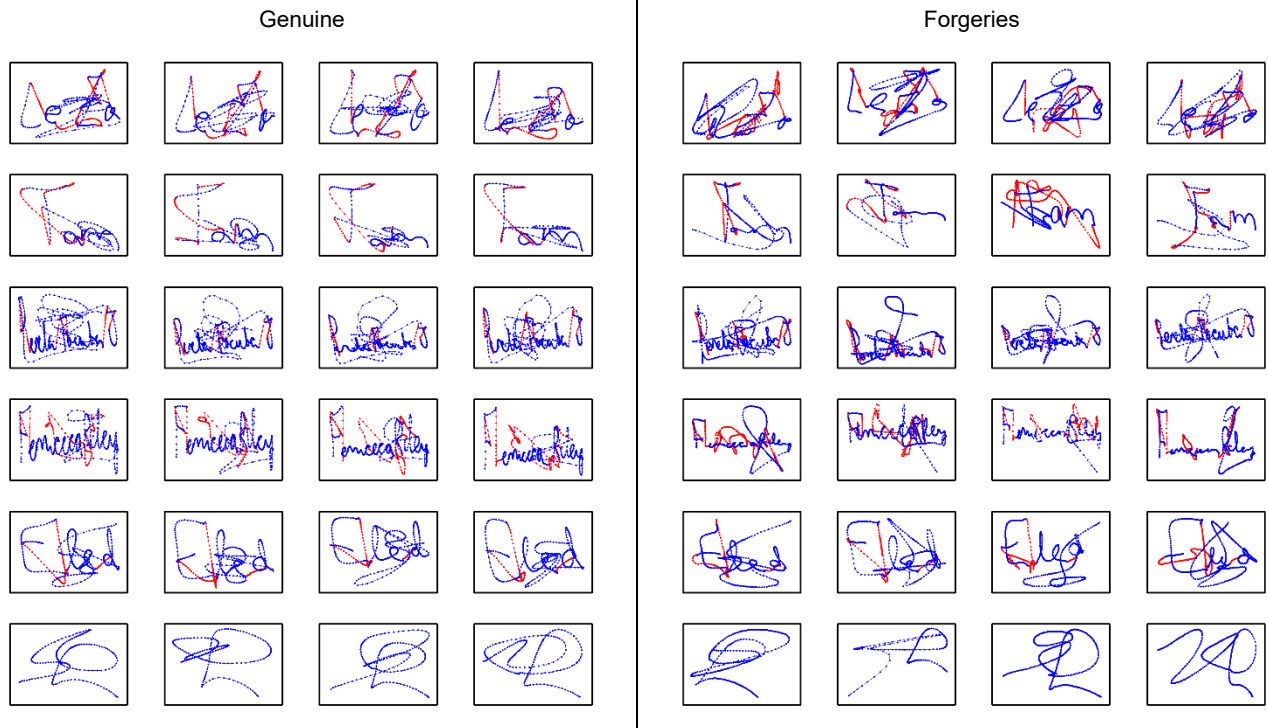


Fig. 10. Examples of intra-personal variability: genuine samples (four columns on the left) and forgeries (four columns on the right)

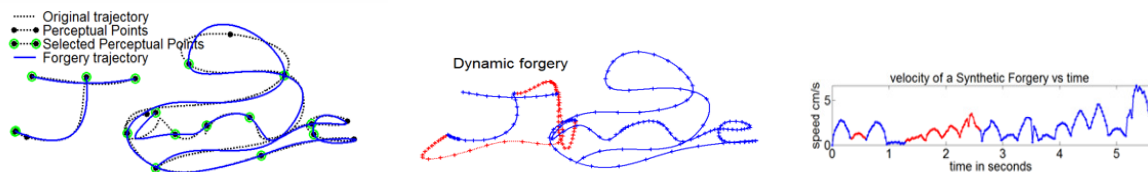


Fig. 11 Left: Example of static signature trajectory (dotted black line) with the most relevant perceptual points marked by black dots, the perceptual points selected by the forger marked with green dots and the interpolated signature trajectory (blue continuous line). Middle: dynamic forgery (blue line with crosses showing the temporal samples) with pen-ups (dotted red line). Right: velocity profile of the forgery.

modify the signature parameters  $\phi$  by changing randomly their value in the range  $[\phi - \phi \times vv, \phi + \phi \times vv]$  [34].

Additionally, it is well known that handwriting evolves during the lifetime of a writer. The relevant factors have been included in the signature synthesizer. Aging has been emulated by reducing the number of nodes in the engram. For instance, the engram for the letter 'a' above defined by {17, 10, 11, 12, 19, 25, 17, 26, 33} (see Fig. 3) would become {17, 11, 12, 19, 25, 17, 33}. An ensemble set of 24 rules has been defined to modify structures such as central loops, upper loops or lower loops in a consistent way for each user. Rules addressing the modification of the ligature between letters and loop directions have also been defined. A random set is applied for each user to keep the handwriting style consistent. As an example, Fig 10 shows several samples generated from master signatures.

## 6.2 Signature imitation

A forgery is the imitation of a person's signature by a third party. A forgery generation method was proposed in [34] on the basis of increasing the intra-writer variability. This procedure usually works well in static signatures but the major drawback of this procedure is that the imitated

velocity profile is too similar to the original. It thus generates forgeries which are not credible.

The procedure proposed in this work tries to emulate the actions of a human forger. Forgers start by examining the signature to be forged. It is supposed that the forger would pay more attention to the most relevant perceptual points of the signature trajectory. Such an idea is incorporated into the forgery generator which identifies the most relevant perceptual points before it interpolates them. These points have been worked out by the procedure proposed at [50] which is based on curvature. The result can be seen at Fig. 11 as black dots on the signature trajectory.

The longer the forger can spend deliberately examining the signature, the more perceptually relevant points he can identify to achieve a better imitation. This process is emulated by detecting as many relevant points as possible and randomly selecting between 70% and 90% of them. This allows us to obtain imitations of different qualities or accuracy. The selected perceptual points set up the stroke limits, thus changing the velocity profile of the genuine signer. The chosen perceptual points can be seen at Fig. 11 marked with green dots.



Although the forger tries to imitate the handwritten style, his cognitive spatial map is different from the genuine signer's. This effect is duplicated by applying a sinusoidal transformation to the relevant perceptual points chosen. A similar transformation has been recently proposed in [21] to duplicate signatures and has also been applied to handwritten CAPTCHA generation [24][25].

The sinusoidal transformation is applied as follows: Let  $x_p$  and  $y_p$  be the coordinates of the perceptual points,  $L_x$  the signature width and  $A_x$  and  $P_x$  the amplitude and period of the  $x$  axis sinusoidal transformation respectively. Let  $L_y$ ,  $A_y$  and  $P_y$  be the corresponding variables for the  $y$  axis sinusoidal transformation. This transformation is defined as  $x_p' = A_x \sin(2\pi A_x x_p / L_x)$  and  $y_p' = A_y \sin(2\pi A_y y_p / L_y)$  where  $x_p'$  and  $y_p'$  are the new coordinates of the perceptual points. For each forged signature, new values of  $L_x$ ,  $A_x$ ,  $P_x$ ,  $L_y$ ,  $A_y$  and  $P_y$  are worked out within their respective margins, which are different for text and flourish.

The trajectory of the imitated signature is calculated by interpolating the perceptually relevant points by a spline. The interpolation spline adjusts the chosen perceptual points plus 5 equidistant points between each pair. The pen-ups are added as mentioned in Section 3.2 but as the hesitation between strokes should be greater because of the uncertainty of the forger, we add more grid points in the source, transition and sink areas of the pen-up trajectory. The results can be seen at Fig. 11.

To sample the trajectory, the velocity is randomly obtained from the distribution given at Sect 4 and the trajectory is lognormal sampled as described in Sect. 5.1. The results are also shown at Fig. 11. In this case, the signature duration is increased from 3.08 s to 5.29 s and it can be seen that the velocity profile is more like that of an imitation. More examples of forgeries are shown at Fig. 10.

## 7 EXPERIMENTS FOR PERFORMANCE EVALUATION

These experiments are aimed at assessing the ability of the synthesizer to produce a wide range of realistic signatures. This is carried out by scoring its ability to generate synthetic datasets that approximate different real corpora such as MCYT330OnLine [39] BiosecureID-Signature UAM subcorpus [40], NISDCC [41][42], SVC 2004 [43], and the two SUSIG subcorpora: Blind and Visual [44]

It is well known that these signature corpora provide different performances since they are acquired with different devices, different protocols and in different geographical regions. Therefore, if for each of the real databases mentioned above, the synthesizer is able to generate a database that is similar to the corresponding real one, it would be proof of its capacity to produce a wide range of intra- and inter-personal variability.

The closeness of two databases with the same morphology can be graded from the similarity between the DET curves obtained with synthetic and real databases. This we obtain through different Automatic Signature Verifiers (ASV) for both random and forgery scenarios with both static and dynamic versions.

Specifically, we selected four classifiers: two off-line and two on-line. The first off-line is based on the Hidden Markov Model (HMM) and geometrical features [51]. The second is a Support Vector Machine (SVM) fed with Local Binary Pattern (LBP) features [52]. The first on-line classifier is based on Dynamic Time Warping (DTW) [53][54] with Euclidean distance and parameter vector given by  $[x, y, p, \partial x, \partial y, \partial p, \partial^2 x, \partial^2 y, \partial^2 p]$  where  $x$  and  $y$  are the sample position and  $p$  the pressure (if it is not available in the real dataset, it is set to 0 for pen-ups and 1 for the rest of the samples). The second on-line classifier [55] is based on the Manhattan distance between histograms of different absolute and relative measures of the signature to be compared.

We chose these four ASVs on the basis of conceptually different features because they are expected to cover a wide range of signature properties and different variability of the signatures.

Each classifier was tested against each dataset with the same configuration since our aim is not to obtain the best result with each dataset but to measure how the synthesizer deals with a wide range of human handwriting variability. Tuning up an ASV for optimum results means to focus on the more stable properties by trying to minimize the influence of the more variable ones. We have used a general configuration so as to consider the different variability sources in a balanced way.

Additionally, all the verifiers are trained by following the same well-established experimental protocol as in [52] in which the training set consists of 5 randomly selected genuine signatures. The remaining genuine signatures are used for testing the false rejection rate. The false acceptance rate for the random impostor experiment has been obtained with the genuine test samples from all the remaining users whereas the false acceptance rate for the deliberate forgeries experiment has been worked out with the forgery samples of each signer. All the experiments are repeated 10 times and the averaged results with their standard deviation are provided in terms of the Equal Error Rates (EERs) and DET curves.

### 7.1 Procedure for generating synthetic datasets with different morphology and performance

Setting up the synthesizer for generating databases that are similar to the real ones is conducted in the following steps. The parameters of the morphology of the real dataset are introduced into the synthesizer. Then we form the variability parameters for generating genuine static, forgery static, genuine dynamic and forgery dynamic signatures to reproduce as closely as possible the performance of the off-line random impostor, off-line deliberate forgeries, on-line random impostor and on-line deliberate forgeries experiments consecutively. This procedure is iteratively repeated looking for the minimum square error between the eight EERs of the real and synthetic dataset.

TABLE I  
PERFORMANCE (ERR IN % AND STD\*) FOR RANDOM IMPOSTOR AND DELIBERATE FORGERIES' EXPERIMENTS

Databases	Random Impostors' experiment				Deliberate Forgeries' experiment			
	Static experiments		Dynamic experiment		Static experiments		Dynamic experiment	
	HMM	SVM	DTW	Man	HMM	SVM	DTW	Man
Real MCYT330OnLine**	3.98 <sub>0.17</sub>	0.55 <sub>0.06</sub>	0.35 <sub>0.08</sub>	2.22 <sub>0.37</sub>	21.43 <sub>0.21</sub>	17.72 <sub>0.45</sub>	4.54 <sub>0.23</sub>	8.76 <sub>0.64</sub>
Synthetic MCYT330OnLine	5.91 <sub>0.42</sub>	1.50 <sub>0.16</sub>	0.41 <sub>0.05</sub>	2.45 <sub>0.27</sub>	27.12 <sub>0.48</sub>	16.68 <sub>0.64</sub>	4.65 <sub>0.24</sub>	2.89 <sub>0.24</sub>
Real BiosecureID-UAM	4.49 <sub>0.34</sub>	1.21 <sub>0.18</sub>	0.23 <sub>0.03</sub>	1.16 <sub>0.17</sub>	26.16 <sub>0.37</sub>	13.24 <sub>0.69</sub>	3.08 <sub>0.21</sub>	1.98 <sub>0.25</sub>
Synthetic BiosecureID	5.46 <sub>0.38</sub>	1.35 <sub>0.19</sub>	0.29 <sub>0.04</sub>	1.49 <sub>0.18</sub>	26.96 <sub>0.44</sub>	16.40 <sub>0.94</sub>	3.48 <sub>0.15</sub>	1.89 <sub>0.21</sub>
Real NISDCC	2.31 <sub>0.92</sub>	0.10 <sub>0.20</sub>	0.36 <sub>0.14</sub>	1.90 <sub>0.23</sub>	14.24 <sub>0.58</sub>	13.03 <sub>1.81</sub>	8.98 <sub>0.33</sub>	4.10 <sub>0.52</sub>
Synthetic NISDCC	3.85 <sub>0.39</sub>	0.67 <sub>0.20</sub>	0.47 <sub>0.13</sub>	1.38 <sub>0.31</sub>	22.56 <sub>0.58</sub>	19.94 <sub>0.58</sub>	5.00 <sub>0.31</sub>	3.21 <sub>0.27</sub>
Real SVC2004**	1.86 <sub>0.25</sub>	0.12 <sub>0.08</sub>	1.07 <sub>0.11</sub>	2.94 <sub>0.45</sub>	6.61 <sub>0.50</sub>	17.25 <sub>0.56</sub>	28.19 <sub>0.63</sub>	15.89 <sub>0.79</sub>
Synthetic SVC2004	2.43 <sub>0.65</sub>	0.02 <sub>0.03</sub>	0.80 <sub>0.14</sub>	0.71 <sub>0.21</sub>	12.18 <sub>0.54</sub>	16.30 <sub>0.67</sub>	23.99 <sub>0.63</sub>	8.30 <sub>0.62</sub>
Real SUSIG Blind**	1.72 <sub>0.36</sub>	0.55 <sub>0.06</sub>	3.19 <sub>0.35</sub>	2.22 <sub>0.37</sub>	14.03 <sub>0.45</sub>	17.72 <sub>0.45</sub>	23.65 <sub>0.56</sub>	8.76 <sub>0.64</sub>
Synthetic SUSIG Blind	2.40 <sub>0.35</sub>	0.16 <sub>0.07</sub>	3.31 <sub>0.22</sub>	0.85 <sub>0.15</sub>	24.54 <sub>0.37</sub>	11.80 <sub>0.96</sub>	13.96 <sub>0.44</sub>	5.90 <sub>0.55</sub>
Real SUSIG Visual**	2.42 <sub>0.31</sub>	0.59 <sub>0.06</sub>	2.12 <sub>0.11</sub>	3.44 <sub>0.34</sub>	14.66 <sub>0.69</sub>	19.56 <sub>0.46</sub>	32.78 <sub>0.44</sub>	8.48 <sub>0.50</sub>
Synthetic SUSIG Visual	3.86 <sub>0.40</sub>	0.67 <sub>0.13</sub>	3.04 <sub>0.10</sub>	1.84 <sub>0.15</sub>	25.66 <sub>1.06</sub>	19.13 <sub>0.59</sub>	17.11 <sub>0.37</sub>	9.03 <sub>0.31</sub>

\* The main value corresponds to the averaged EER whereas the sub index appertains to the standard deviation

\*\* Static signatures generated from the dynamic signatures through the ink deposition model

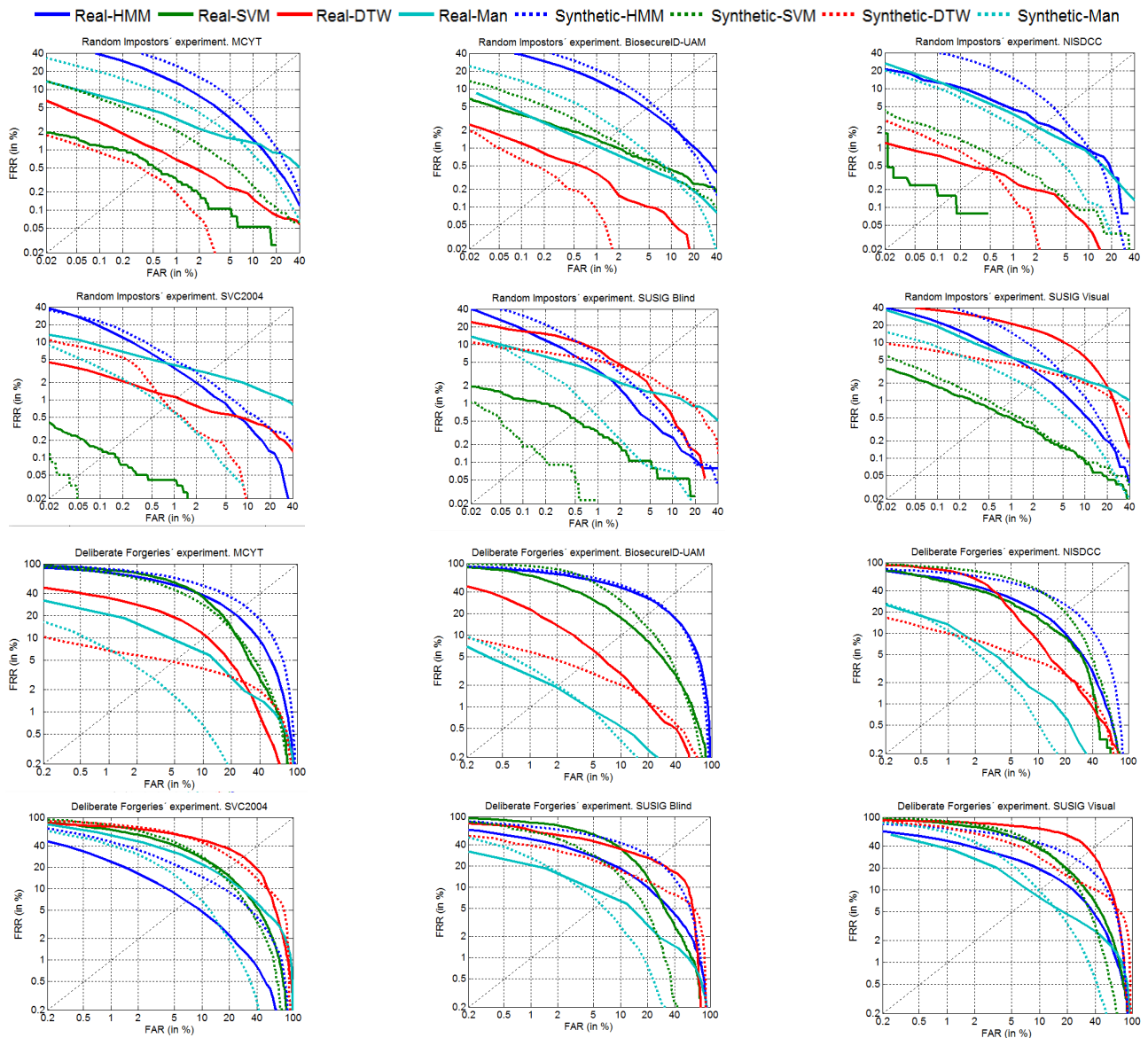


Fig 12. DET Curves for all the experiments. The solid lines represent the real databases whereas the dotted line refers to synthetic datasets. HMM classifier DET curves are depicted in blue, SVM in green, DTW in red and Manhattan in cyan colour.

TABLE II  
AREA BETWEEN DET CURVES OF REAL AND SYNTHETIC DATABASES

Database	Random Impostors' experiment					Deliberate Forgeries' experiment				
	Static experiments		Dynamic experiment		mean	Static experiments		Dynamic experiment		mean
	HMM	SVM	DTW	Man		HMM	SVM	DTW	Man	
MCYT330OnLine*	0.0072	0.0013	0.0007	0.0045	0.0014	0.0667	0.0166	0.0252	0.0243	0.0332
BiosecureID-UAM	0.0042	0.0008	0.0002	0.0015	0.0016	0.0141	0.0345	0.074	0.0011	0.0309
NISDCC	0.0040	0.0004	0.0001	0.0024	0.0017	0.0738	0.0623	0.0283	0.0420	0.0516
SVC2004	0.0016	0.0001	0.0017	0.0088	0.0030	0.0394	0.0158	0.0351	0.0642	0.0386
SUSIG Blind	0.0015	0.0002	0.0031	0.0056	0.0026	0.0887	0.0539	0.0760	0.0150	0.0584
SUSIG Visual	0.0040	0.0002	0.0127	0.0920	0.0272	0.1022	0.0205	0.1564	0.0207	0.0749
mean	0.0037	0.0005	0.0030	0.0258		0.0641	0.0339	0.0658	0.0278	

\*Refers to the area between the DET curve of the real MCYT330OnLine Dataset and the DET curve of its synthetic version

This procedure is based on the hypothesis that 1) the parameters used for generating the dynamics of the signature do not affect the performance of the static signature, but the opposite does not apply and 2) the parameters to generate genuine samples modify the performance of the deliberate forgeries experiment, but not the opposite.

## 7.2 Similarity between real databases and their synthetic counterparts

This section measures the similarity between the real datasets and their synthetic versions. Table I provides the EERs obtained with real and their corresponding synthetic datasets. It can be seen that the synthesizer is capable of generating a wide range of synthetic databases with different performances.

Additionally, in the synthetic datasets, the fact that there are different relations between the EERs of the random impostors and deliberate forgery experiments tells us that it is possible to generate forgeries with different skill levels. The ability of changing the relation between the EERs of static and dynamic experiments shows the possibility of modulating the dynamic variability in different ways.

Obviously, given the wide and unpredictable nature of the human behavior found in the five analyzed datasets, the match between real and synthetic datasets can be improved, e.g. in the SUSIG Visual database. The model proposed in this work focuses on the neuromotor characteristics of the signature while other factors related to operational conditions should be included, e.g. acquisition sensor characteristics, different languages, mobile acquisition and so on.

Similarities and differences between real and synthetic datasets are analyzed in Fig. 12 and Table II. Fig. 12 shows the Detection Error Tradeoff (DET) curves of all the experiments. It can be seen that there exist intersections between DET curves of real and synthetic datasets, which means that there is room for emulating the complete variability of real databases.

A numerical score of DET curves similarities and differences is given in Table II which shows the area between the DET curves of each dataset and its synthetic version. As can be seen in the *mean* column for the random

impostors' experiment in Table II, MCYT330OnLine, BiosecureID and NISDCC datasets are the best replicated, which correspond to Western datasets acquired with WACOM tablets. However, SVC2004, performed by Chinese people, and SUSIG databases, acquired with touch devices, are the worse matched. In the case of deliberate forgeries, the MCYT330OnLine, BiosecureID and SVC2004 forgers are the best imitated.

Concerning the classifiers, the *mean* row in Table II suggests that the easiest datasets to emulate in the random impostors' experiment are the SVM and the DTW for off-line and on-line cases respectively. In the deliberate forgery experiments we use the SVM and the Manhattan-based for off-line and on-line cases respectively.

These results suggest, among others, the need for deeper studies in human handwriting variability in: 1) non-Western writers and 2) touch devices. Although a full model of a human variability is far away from the current technology, it is expected both such studies would provide a step forward in its understanding.

## 7.3 Comparison with other synthesizers

The proposed synthesizer was compared with the state of the art systems proposed in [28] and [56]. Specifically, [28] proposes an on-line synthesizer of flourish like signatures without text, forgeries or pen-ups. This on-line dataset is converted into off-line in [56] using the same ink deposition model used in [34]. The performance is evaluated in [28] and [56] with the same HMM, SVM and DTW classifiers that this paper uses.

To compare those results with ours as fairly as possible, we have generated with our procedure a dataset without text, forgeries or pen-ups to simulate the MCYT330OnLine dataset.

Table III shows the comparative training with 5 samples. It includes the baseline given by [29] and [48] with the MCYT330OnLine dataset, their results and our results. Unlike the procedure proposed in [28] and [56], our synthesizer is capable of generating synthetic samples which meet, with a low margin of error, the performance of real MCYT330OnLine signatures.

## 7.4 Computational cost

The computational costs in terms of averaged execution time of running these algorithms in Matlab® with an Intel® Core™ i7-4790 CPU @ 3.60GHz are as follows: to generate the synthetic identity: 0,9 sec., to generate a genuine sample: 1.3 sec. and to generate a forgery: 1.0 sec. The longest time for the most complex signatures generated in the dataset are 1.1 sec., 1.6 sec. and 1.2 sec. respectively.

## 8. CONCLUSION

This paper proposes a novel and unified method for synthetic signature generation of both the static signature image and its dynamic sequences of synthetic identities using a unique signature synthesizer framework. Additionally, the proposed framework is able to synthesize realistic forgeries based on a human plan to imitate handwriting.

The generation method is inspired by both the human cognitive and neuromotor model perspectives. Specifically, it is based on the equivalence model theory that defines the handwriting action into two steps: the action plan and the neuromotor inverse model. Following this model, the ballistic signature trajectory is built with an inertial filter, which represents the neuromuscular system. Then, the action plan is simulated by a polygon through a hexagonal spatial grid. For static representation, an ink deposition model is applied whereas for dynamic representation, the sampling points are obtained by lognormal sampling of the trajectory.

Several synthetic datasets with different lexical and morphological properties and performances have been used to assess the ability of the synthesizer to handle a wide range of varied sources. All of them are freely available at <http://www.gpds.ulpgc.es/download/>.

The proposed algorithm has enormous potential since it provides a deeper analysis of the method of producing handwriting which is demanded by many experts such as neurologists, graphologists and forensic and computer scientists. For instance, in computer science and biometrics it make it easier to address topics such as aging, interoperability, multiscript, scalability and template protection, etc. at only minor computational cost, once the synthesizer setup is established.

Additionally, inverting the model, i.e. obtaining the grid map that imitates the cognitive map and the smoothing filters that represent the motor inertia, can help to evaluate some learning problems for children or cognitive and motor degenerative problems such as Parkinson's or Alzheimer's diseases at early stages [10][11][12].

These inverse parameters can also be combined with the usual forensic science features [6] to evaluate the authenticity of handwritten signatures in contracts, testaments, corporate tax returns, etc. A similar approach can be applied to graphology.

Finally, the lack of large real data sets is one of the key barriers for the use of deep learning algorithms [57] on signature applications so synthetic databases will be useful

TABLE III  
COMPARISON WITH OTHER SYNTHESIZERS

Random Impostors' experiment (MCYT330 on-line dataset)			
Systems	HMM	SVM	DTW
[28] and [56] baseline with MCYT	5.30	0.35	0.44
[28][56] synthetic signatures	4.28	3.64	0.17
Our baseline with real MCYT	3.98	0.55	0.35
Our results for emulating MCYT in [28] and [56] conditions	4.01	0.63	0.37

resources for the research community. With this work, we make publicly available several datasets which comprise more than 10,000 signatures that can be used to train either statistical learning approaches or new deep architectures.

This paper suggests several future research lines, currently being worked on, such as multiscript generation, to produce real signature duplicates, and the reversion of this method to obtain the grid and inertia filters for health and educational applications.

## Acknowledgment

This study was funded by the Spanish government's MIMCO TEC2012-38630-C04-02 research project and European Union FEDER program/funds.

## REFERENCES

- [1] A. Marcelli, A. Parziale and A. Santoro, "Modelling Visual Appearance of Handwriting", in *17th International Conference on Image Analysis and Processing*, Italy, 2013.
- [2] A. K. Jain, A. A. Ross and K. Nandakumar, *Introduction to Biometrics*, Springer, 2011.
- [3] D. Impedovo and G. Pirlo, "Automatic Signature Verification: The State of the Art", in *IEEE Transactions on Systems, Man, and Cybernetics, Part C: Applications and Reviews*, vol. 38, no. 5, pp. 609-635, September 2008.
- [4] M. Diaz-Cabrera, A. Morales and M. A. Ferrer. "Emerging Issues for Static Handwritten Signature Biometric", in *Emerging Aspects in Handwritten Signature Processing*, Edited by Giuseppe Pirlo, Donato Impedovo and Michael Fairhurst, Word Scientific Publishing Co. Pte. Ltd. London, pp. 111-122, 2014.
- [5] J. Galbally, M. Diaz-Cabrera, M. A. Ferrer, M. Gomez-Barrero, A. Morales and J. Fierrez, "On-Line Signature Recognition Through the Combination of Real Dynamic Data and Synthetically Generated Static Data", *Pattern Recognition*, vol. 48, pp. 2921-2934, September 2015.
- [6] C. Bird, B. Found, K. Ballantyne and Doug Rogers, "Forensic Handwriting Examiners' Opinions on the Process of Production of Disguised and Simulated Signatures", in *Forensic Science International*, vol. 195, no. 1-3, pp. 103-107, 2010.
- [7] A. M. Wing, "Motor Control: Mechanisms of Motor Equivalence in Handwriting", in *Current Biology*, vol. 10, pp. 245-248, 2000.
- [8] M. Djoua and R. Plamondon, "A New Algorithm and System for the Characterization of Handwriting Strokes with the Delta-Lognormal Parameter", in *IEEE Transactions on Pattern Analysis and Machine Intelligence*, vol. 31, no. 11, pp. 2060-2072, 2009.
- [9] C. O'Reilly and R. Plamondon, "Impact of the Principal Stroke Risk Factors on Human Movements", in *Human Movements Science*, vol. 30, no. 4, pp. 792-806, 2011.
- [10] C. O'Reilly and R. Plamondon, "Design of A Neuromuscular Disorders Diagnostic System Using Human Movement



- Analysis", in *Proceedings on Information Science, Signal Processing and their Applications*, pp. 787-792, Quebec, Canada, 2012.
- [11] T. E. Eichhorn, T. Gasser, N. Mai, C. Marquardt, G. Arnold, J. Schwarz and W.H. Oertel, "Computational Analysis of Open Loop Handwriting Movements in Parkinson's Disease: A Rapid Method to Detect Dopaminergic Effects", in *Movement disorders*, vol. 11, n. 3, pp. 289-297, 1996.
- [12] J. Neils-Strunjas, K. Groves-Wright, P. Mashima, and S. Harnish, "Dysgraphia in Alzheimer's Disease: A Review for Clinical and Research Purposes", in *Journal of Speech, Language, and Hearing Research*, vol. 49, no. 6, pp. 1313-1330, 2006.
- [13] Helmut Ploog, *Handwriting Psychology: Personality Reflected in Handwriting*, iUniverse, 2013.
- [14] M. Rejman-Greene, "Privacy Issues in the Application of Biometrics: A European Perspective", in *Biometric Systems. Technology, Design and Performance Evaluation*, Springer, pp.335-359, 2005.
- [15] E. Frias-Martinez, A. Sanchez and J. Velez, "Support Vector Machines versus Multi- Layer Perceptrons for Efficient Off-Line Signature Recognition", *Engineering Applications of Artificial Intelligence*, vol. 19, no. 6, pp. 693-704, September 2006.
- [16] J. Galbally, J. Fierrez, M. Martinez-Diaz and J. Ortega-Garcia, "Improving the Enrollment in Dynamic Signature Verification with Synthetic Samples", in *Proceedings of the IAPR International Conference on Document Analysis and Recognition*, pp. 1295-1299, Barcelona, Spain 2009.
- [17] R. Plamondon, C. O'Reilly, J. Galbally, A. Almaksour and E. Anquetil. "Recent Developments in the Study of Rapid Human Movements with the Kinematic Theory: Applications to Handwriting and Signature Synthesis", in *Pattern Recognition Letters*, vol. 35, pp. 225-235, 2014.
- [18] A. Fischer, R. Plamondon, C. O'Reilly and Y. Savaria, "Neuromuscular Representation and Synthetic Generation of Handwritten Whiteboard Notes", in *Proceedings of the International Conference on Frontiers in Handwriting Recognition*, pp. 222-227, Greece, September 2014.
- [19] M Diaz, A. Fischer, R. Plamondon and M. A. Ferrer, "Towards an Automatic On-Line Signature Verifier Using Only One Reference per Signer", in *13th International Conference on Document Analysis and Recognition*, Nancy, France, 23-26th August, 2015.
- [20] C. Rabasse, M. Guest and C. Fairhurst, "A New Method for the Synthesis of Signature Data With Natural Variability", in *IEEE Transactions on System, Man, and Cybernetics – Part B*, vol. 38, no. 3, June 2008.
- [21] M. Diaz-Cabrera, M. A. Ferrer and A. Morales Moreno, "Cognitive-Based Model to Generate Duplicated Static Signature Images", in *14th International Conference on Frontiers in Handwriting Recognition*, pp. 61-66, Greece, September, 2014.
- [22] I. Guyon, "Handwriting Synthesis from Handwritten Signatures", in *Proceedings of the Fifth International Workshop on Frontiers of Handwriting Recognition*, pp. 309-312, 1996.
- [23] A. Lin and L. Wang, "Style-Preserving English Handwriting Synthesis", in *Pattern Recognition*, vol. 40 pp. 2097-2109, 2007.
- [24] A. O. Thomas, A. Rusu and V. Govindaraju, "Synthetic Handwritten CAPTCHAs", in *Pattern Recognition*, vol. 42, no.12, pp. 3365-3373, December 2009.
- [25] U. Midić, "Automatic Generation of Synthetic Handwriting Samples with Application to CAPTCHA", in *Computer Information Science Department Report*, Temple University, December 2014.
- [26] D. V. Popel, "Signature Analysis, Verification and Synthesis in Pervasive Environments", in *Synthesis and Analysis in Biometrics*, World Scientific, pp. 31-63, 2007.
- [27] J. Galbally, R. Plamondon, J. Fierrez and J. Ortega-Garcia, "Synthetic On-Line Signature Generation. Part I: Methodology and Algorithms", in *Pattern Recognition*, vol. 45, pp. 2610-2621, July 2012.
- [28] J. Galbally, J. Fierrez, J. Ortega-García and R. Plamondon, "Synthetic On-Line Signature Generation. Part II: Experimental Validation", in *Pattern Recognition*, vol. 45, pp. 2622-2632, July 2012.
- [29] R. Plamondon, "A Kinematic Theory of Rapid Human Movements. Part I: Movement Representation and Generation", in *Biological Cybernetics*, vol. 72, no. 4, pp 295-307, March 1995.
- [30] R. Plamondon, "A Kinematic Theory of Rapid Human Movements. Part II: Movement Time and Control", in *Biological Cybernetics*, vol. 72, no. 4, pp. 309-320, March 1995.
- [31] R. Plamondon, "A Kinematic Theory of Rapid Human Movements. Part III: Kinematic Outcomes", in *Biological Cybernetics*, vol. 78, no. 2, pp. 133-145, February 1998.
- [32] R. Plamondon, "A Kinematic Theory of Rapid Human Movements. Part IV: A Formal Mathematical Proof and New Insights", in *Biological Cybernetics*, vol. 89, no. 2, pp. 126-138, August 2003.
- [33] M. A. Ferrer, M. Díaz-Cabrera, A. Morales, "Synthetic Off-line Signature Image Generation", *Proceedings of 6th IAPR International Conference on Biometrics*, Madrid, Spain, pp. 1-7, June 2013.
- [34] M. A. Ferrer, M. Diaz, A. Morales, "Static Signature Synthesis: A Neuromotor Inspired Approach for Biometrics," in *IEEE Transactions on Pattern Analysis and Machine Intelligence*, vol. 37, no.3, pp.667-680, March 2015.
- [35] A. Marcelli, A. Parziale nad R. Senatore, "Some Observations on Handwriting from a Motor Learning Perspective", in *2nd workshop on Automated Forensic Handwriting Analysis*, Washington DC, USA, August 2013.
- [36] G. Gandadhar, "A Neuromotor Model of Handwriting Generation: Highlighting the role of Basal Ganglia", *Thesis submitted at Department of Electrical Engineering, Indian Institute of Technology, Madras*, April 2006.
- [37] M. Kawato, "Internal Models For Motor Control And Trajectory Planning," in *Current Opinion in Neurobiology*, vol. 9, pp. 718-727, 1999.
- [38] M. Díaz, M.A. Ferrer and A. Morales, "Modeling the Lexical Morphology of Western Handwritten Signatures", in *PLOS ONE*, vol. 10, no. 4, pp.1-22, April 2015.
- [39] J. Ortega-Garcia, J. Fierrez-Aguilar, D. Simon, J. Gonzalez, M. Faundez, V. Espinosa, A. Satue, I. Hernaez, J. J. Igarza, C. Vivaracho, D. Escudero and Q. I. Moro, "MCYT Baseline Corpus: A Bimodal Biometric Database", in *IEE Proceedings Vision, Image and Signal Processing*, Special Issue on Biometrics on the Internet, vol. 150, no. 6, pp. 395-401, December 2003.
- [40] J. Fierrez, J. Galbally, J. Ortega-Garcia, et al., "BiosecureID: A Multimodal Biometric Database", in *IEEE Proceedings on Pattern Analysis and Applications*, vol. 13, no. 2, pp. 235-246, May 2010.
- [41] V. Blankers, C. Heuvel, K. Franke and L. Vuurpijl, "Signature Verification Competition", in *10th International Conference on Document Analysis and Recognition*, pp. 1403-1407, Barcelona, Spain, 2009.
- [42] L. Alewijnse, C. Van Den Heuvel, R. Stoel and K. Franke, "Analysis of Signature Complexity", in *Proceedings of the 14th Biennial Conference of the International Graphonomics Society: Advances in Graphonomics*. pp. 6-9, 2009.
- [43] "SVC2004: First international Signature Verification Competition", in *Lecture Notes in Computer Science: Biometric Authentication*, Ed. by D. Zhang and A. Jain, vol. 3072, pp. 16-22, Springer, Berlin Heidelberg, 2004.

- [44] A. Kholmatov and B. Yanikoglu, "SUSIG: an on-Line Signature Database, Associated Protocols and Benchmark Results", in *Pattern Analysis and Applications*, vol. 12, pp. 227-236, 2009.
- [45] T. Hafting, M. Fyhn, S. Molden, M. Moser and E. I. Moser, "Microstructure of a Spatial Map in the Entorhinal Cortex", in *Nature*, vol. 436, pp. 801-806, August 2005.
- [46] T. F. Cootes, C. J. Taylor, D. H. Cooper, J. Graham, "Active Shape Models – Their Training and Application", in *Computer Vision and Image understanding*, vol. 61, no. 1 pp. 38-59, January 1995.
- [47] D. Farina and R. Merletti, "Comparison of Algorithms for Estimation of EMG Variables During Voluntary Iso-Metric Contractions", in *Journal of Electromyographic Kinesiology*, vol.10, 2000.
- [48] M. A. Ferrer, M. Diaz-Cabrera, A. Morales, J. Galbally and M. Gomez-Barrero, "Realistic Synthetic Off-line Signature Generation Based on Synthetic On-line Data", in *Proceedings of IEEE International Carnahan Conference on Security Technology*, pp. 116-121, Medellin, Colombia, October 2013.
- [49] C. O'Reilly and R. Plamondon, "Development of a Sigma-Lognormal Representation for On-Line Signatures", in *Pattern Recognition*, vol. 42, no. 12, pp. 3324-3337, December 2009.
- [50] J. J. Brault and R. Plamondon, "Segmenting Handwritten Signatures at their Perceptually Important Points", in *IEEE Transactions on Pattern Analysis and Machine Intelligence*, vol. 15, no. 9, pp. 953-957, 1993.
- [51] M. A. Ferrer, J. B. Alonso and C. M. Travieso, "Offline Geometric Parameters for Automatic Signature Verification using Fixed-Point Arithmetic", in *IEEE Transactions on pattern analysis and machine intelligence*, vol. 27, no. 6, pp. 993-997, June 2005.
- [52] M. A. Ferrer, F. Vargas, A. Morales and A. Ordoñez, "Robustness of Off-line Signature Verification Based on Gray Level Features", in *IEEE Transactions on Information Forensics and Security*, vol. 7, no. 3, pp. 966-977, June 2012.
- [53] A. Kholmatov and B. Yanikoglu, "Identity Authentication using an Improved Online Signature Verification Method", in *Pattern Recognition Letters*, vol. 26, pp. 2400-2408, 2005.
- [54] A. Fischer, M. Diaz, R. Plamondon, M. A. Ferrer, "Robust Score Normalization for DTW-Based On-Line Signature Verification", in *13th International Conference on Document Analysis and Recognition*, Nancy, France, August, 2015.
- [55] N. Sae-Bae and N. Memon, "Online Signature Verification on Mobile Devices" in *IEEE Transactions on Information Forensics and Security*, vol. 9, no. 6, pp. 933-947, June 2014.
- [56] M. Diaz, M. Gomez-Barrero, A. Morales, M. A. Ferrer and J. Galbally, "Generation of Enhanced Synthetic Off-Line Signatures Based on Real On-Line Data", in *Proceedings of 14th International Conference on Frontiers in Handwriting Recognition (ICFHR)*, pp.482-487, September 2014.
- [57] Y. LeCun, Y. Bengio, G. Hinton, "Deep learning". In *Nature*, vol. 521, no.7553, pp. 436-444, 2015.



**Miguel A. Ferrer** received the M.Sc. degree in telecommunications, in 1988, and his Ph.D. degree, in 1994, each from the Universidad Politécnica de Madrid, Spain. He belongs to the Digital Signal Processing research group (GPDs) of the research institute for technological development and Communication Innovation (IDeTIC) at the University of Las Palmas de Gran Canaria in Spain where since 1990 he has been an Associate Professor. His research interests lie in the fields of computer vision, pattern recognition, biometrics, mainly those based on hand and handwriting, audio quality, mainly for health and condition machinery evaluation and vision applications to fisheries and aquaculture.



**Moises Diaz-Cabrera** received two M. Tech degrees in 2010: Industrial Engineering and Industrial Electronics and Automation Engineering and holds a M.Sc. in Intelligent Systems and Numerical Applications in Engineering (2011) as well as a M.Ed. in Secondary Education (2013), all from La Universidad de Las Palmas de Gran Canaria. He is currently pursuing a Ph.D. degree and his research areas include handwritten signature recognition, pattern recognition and vision applications to Intelligent Transportation Systems. He has been a visiting student researcher at the Vislab group, at the University of Parma in Italy, the University of Bari in Italy, the École Polytechnique de Montréal in Canada, the University of Fribourg in Switzerland and the Indian Statistical Institute, Kolkata.



**Cristina Carmona-Duarte** received the Telecommunication Engineering degree in 2002 and of Ph.D. degree in 2012 from Universidad de Las Palmas de Gran Canaria. She has been an Assistant Professor at Universidad de Las Palmas and she is currently researcher. Her research areas include high resolution radar, pattern recognition and biometrics.



**Aythami Morales Moreno** received his M.Sc. degree in Telecommunication Engineering in 2006 from Universidad de Las Palmas de Gran Canaria. He received his Ph.D degree from La Universidad de Las Palmas de Gran Canaria in 2011. He performs his research works in the ATVS - Biometric Recognition Group at Universidad Autónoma de Madrid and he has performed research stays at the Biometric Research Laboratory at Michigan State University, the Biometric Research Center at Hong Kong Polytechnic University and the Biometric System Laboratory at University of Bologna. His research interests are focused on pattern recognition, computer vision, machine learning and biometrics signal processing. He is author of more than 60 scientific articles published in international journals and conferences. He has received awards from ULPGC, La Caja de Canarias, SPEGC, and COIT. He has participated in 7 National and European projects in collaboration with other universities and private entities such as UAM, UPM, EUPM, Indra, Unión Fenosa, Soluziona.